The Graphene Sensor Technology

Tarun M Radadiya

Student of Electronics & Communication Department of Vadodara institute of engineering, Gujarat Technological University (GTU), Vadodara, Gujarat, India

Abstract: ***Graphene has emerged as one of the strongest candidates for post-silicon technologies. One of the most important applications of graphene in the foreseeable future is sensing of particles of gas molecules, bio-molecules or different chemicals or sensing of radiation of particles like alpha, gamma or cosmic particles. Several unique properties of graphene such as its extremely small thickness, very low mass, large surface to volume ratio, very high absorption coefficient, high mobility of charge carriers, high mechanical strength and high Young's modulus make it exceptionally suitable for making sensors. Graphene based materials have considerable attention for the fabrication of non-enzymatic sensors due to their low cost, high catalytic ability and good stability use in sensor technology.***

Keyword: Graphene properties, sensors, manufacturing technology

1. Introduction

Graphene has been extensively investigated for the development of optoelectronic devices, super capacitors and various types of high performance sensors, due to its large surface-to-volume ratio, unique optical properties, excellent electrical conductivity, remarkably high carrier mobility (in excess of 20000 cm^{2}V-1s^{-1}), high carrier density(1013 cm^{-2}), high thermal conductivity, room temperature ,Hall effect, ambipolar field-effect characteristics, high signal-to-noise ratio (due to low intrinsic noises), and extremely high mechanical strength (200 times greater than steel, tensile modulus of 1 TPa).

The large surface area of graphene enhances the surface loading of desired biomolecules, either through passive adsorption, or by covalent crosslinking to the reactive groups of biomolecules. On the other hand, the excellent conductivity and small band gap of graphene are beneficial for the conduction of electrons between the biomolecules and the electrode surface. Graphene has about two-fold higher effective surface area and greater cost-effectiveness than carbon nanotubes. Additionally, it has greater homogenous surface that is responsible for highly uniform and efficient functionalization higher elasticity than membrane materials like silicon nitride commonly used in NEMS [1].

Graphene is another class of carbon based material. It has a two-dimensional (2D) network of SP2 hybridized carbon atoms packed into a hexagonal structure, and recently, it has become a potential candidate for strain sensor because of its good mechanical properties [1]. Enormous efforts have been devoted to exploration of its many applications in the field of science and engineering [2–6]. Graphene is novel material all properties of graphene excellent, sensor technology graphene excellent response very high performs, sensitive nearly 100% accurate, efficient sensor are manufacture.

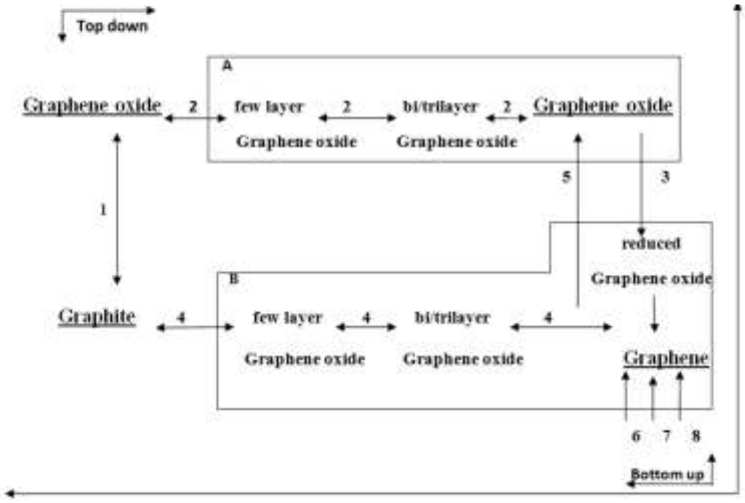

Figure 1: Classification of graphene family materials.
X axis - Number of layers
Y axis - Oxidation layer

(1) Oxidation of graphite to graphite oxide according to the Hummers, Staudenmeier or Brodie method [10]. (2) Stepwise exfoliation of graphite oxide to give graphene oxide in aqueous colloidal suspensions by sonication and stirring [10].(3) Reduction of graphene oxide by chemical reactions [28], thermal annealing [14], flash reduction [15], enzymatic reduction [16] or electrode position [12]. (4) Mechanical exfoliation of graphite to give graphene (tape method)[19]. (5) Oxidation of graphene sheets to graphene oxide. (6) Thermal decomposition of a SiC wafer [8]. (7) Growth of graphene films by chemical vapor deposition [9]. (8) Total synthesis routines with precursor molecules [11, 13, 17, 18]. Group A includes graphene materials primarly used for their electronic properties, group B for their optical properties.

2. Graphene Biosensor

The detection of biologically active molecules is of critical importance from a biomedical, environmental, and security point of view. Such detection can be carried out by biosensor or by bio analytical protocols. A chemical sensor is a device that quantitatively or semi quantitatively converts information about the presence of a chemical species to an analytically useful signal [20]. Sensors consist of two elements: a receptor and a transducer (Figure. 2). A receptor can be any organic or inorganic material with (preferably) a specific interaction with one analyte or group of analytes. In the case of biosensors, the recognition element is a bio molecule. The second key element of the sensing platform is

Licensed Under Creative Commons Attribution CC BY

the transducer, which converts chemical information into a measurable signal. Bio analytical protocols usually include more than one processing step. In this review, we will describe biosensors and bio analytical systems that utilize graphene as a key component.

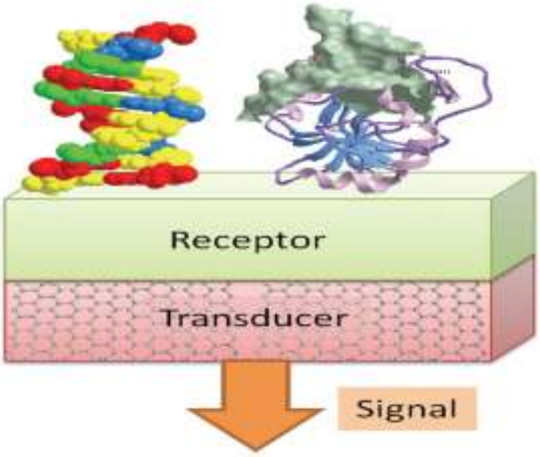

Figure 2: Scheme of a biosensor. The biosensor consists of a receptor layer, which consists of a bio molecule (e.g., DNA or protein), and a transducer, which is a graphene-based material.

Neither CVD-produced graphene nor mechanically exfoliated graphene contain large quantities of defects or functionalities. However, bulk quantities of graphene-based nanomaterials are typically prepared by different methods, such as the thermal exfoliation of graphite oxide [21] which leads to a material called thermally reduced graphene (TRGO) or, for example, sono-assisted exfoliation of graphite oxide to graphene oxide (GO) [22]. Graphene oxide can be further reduced chemically or electrochemically. Thermally reduced graphene oxide (TRGO) contains large amounts of defects and significantly differs from pristine graphene, which has a perfect honeycomb lattice structure [23]. The presence of the defects is not disadvantageous. To the contrary, it is well known that heterogeneous electron transfer in the electrochemistry of sp2 carbons occurs at the edges and defects, and not at the basal plane of graphene sheets [24]. Graphene oxide has a structure that is not fully planar because the sp2 carbon network is heavily damaged. It contains large amounts of oxygen-containing groups, which can be beneficial to the functionalization through the action of the biomolecules for bio recognition events during biosensing [22]. Graphene oxide can be chemically or electrochemically reduced. Such products have a partly restored sp2 lattice that also contains some degree of oxygen-bearing groups. The products are typically referred to as chemically reduced graphene oxide (CRGO) or electrochemically reduced graphene oxide (ERGO) [25].

3. Graphene in Electrochemical Biosensors

Electrochemical detection is highly sensitive to electro active molecules. In addition to sensitivity (which is also a property of electrical detection), it also offers detection selectivity as different molecules can be oxidized/reduced at different potentials. Graphene is an excellent Conductor of electrical charge. Heterogeneous electron transfer (the transfer of electrons between graphene and the molecule in the solution necessary for the oxidation/reduction of said molecule) occurs at the edges of the graphene or at defects in the basal plane.

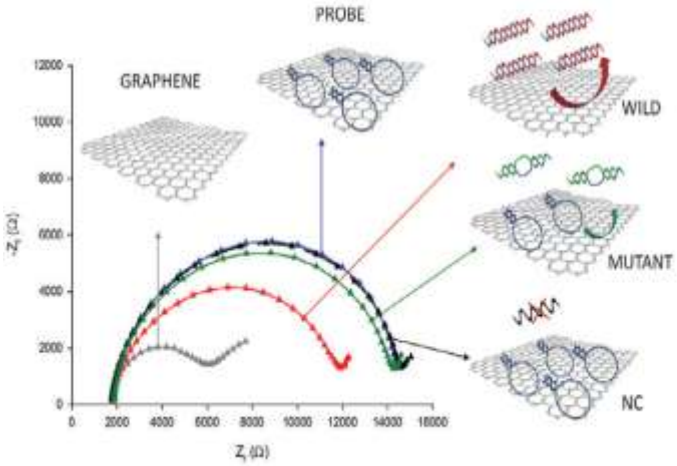

Figure 3: Impedimetric biosensor based on a graphene platform for Hairp in DNA based detection

Schematic of the protocol and Nyquist plots, -Zi vs. Zr, of the graphene surface (gray), hpDNA (blue), complementary target (red), 1-mismatch target (green), and negative control with a non-complementary sequence (black) (concentration of DNA probes, 1 × 10-5 M; concentration of DNA target, 3 × 10-8 M). All measurements were performed in 0.1 M PBS buffer solution containing 10 mM K3 [Fe(CN)6]/K4 [Fe(CN)6][26].

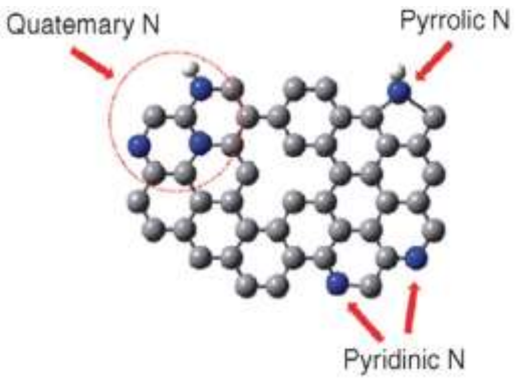

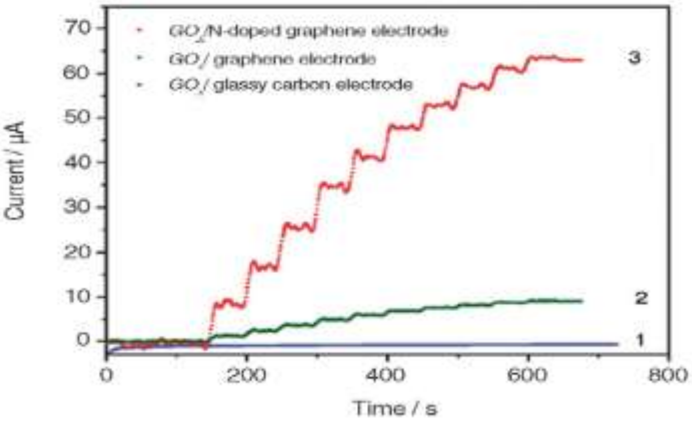

Licensed Under Creative Commons Attribution CC BY

Figure 4: N-doped graphene for electrochemical biosensing. (a) Schematic representation of N-doped graphene. Gray for the carbon atom, blue for the nitrogen atom, and white for the hydrogen atom. A possible defect structure is shown in the middle of the ball-stick model. (b) Current-time curves for GOx immobilized on (1) a glassy carbon electrode, (2) a graphene electrode, and (3) A N-doped graphene electrode with the successive addition of 0.1 mM glucose.

Thus, the high surface area of graphene facilitates large amounts of defects and thus, electro active sites [27]. Graphene has been employed in many schemes for sensing glucose[28]. This is reflected by the fact that electrochemistry is paramount to sensing glucose for diabetic patients (reflected by the multibillion USD gluco sensing market) [29]. The glucose oxidase enzyme is used as a bio recognition element glucose oxidase oxidizes glucose to gluconic acid and shuffles electrons into the oxygen which is dissolved in the solution, and then reduced to hydrogen peroxide. Hydrogen peroxide is typically detected electrochemically. However, in several examples, direct electron transfer from the enzyme (without the need of O_2 as an electron acceptor) is possible, making this an analytically valuable sign al[29]. Ultrathin multilayer graphene platelets (also called graphite nanoplatelets) have been used as a transducing material for the biosensing of glucose[30].

Table 1: Summary of relevant quantitative parameters of selected sensors and biosensors Analyte

Analyte	Electrode material	Limit of detection	Linear range	Ref.
Pb^{2+}	Glucose	0.02 µg/L	0.5–50 µg/L	[39]
cd^{2+}	Glucose	0.02 µg/L	1.5–30 µg/L	[39]
H_2O_2	Graphene/AuNPs/chitosan	180 µM	0.2–4.2 mM	[47]
H_2O_2	Reduced graphene oxide	0.05 µM	0.01–10 mM	[38]
Dopamine	Glucose	NA	5–200 µM	[40]
Dopamine	Glucose	2.64 µM	4–100 µM	[41]
NADH	Ionic liquid-graphene	5 µM (ethanol)	0.25–2 mM	[42]
Glucose	Graphene/Au/Nafion	5 µM	0.015–5.8 mM	[46]
Glucose	Reduced graphene oxide	2 µM	0.01–10 mM	[38]
Glucose	Graphite nanosheet/Nafion	NA	0.2–1.4 mM	[43]
Glucose	N-doped graphene	0.01 mM	0.1–1.1 mM	[44]
Glucose	Graphene oxide	1 µM	1–20 µM	[45]

In another example, it was shown that N-doped graphene provides significantly enhanced oxidation currents for the enzymatic detection of glucose, compared to ordinary graphene materials (Figure. 4). [32]. Direct electron transfer from glucose oxidase has been reported by several authors. Glucose oxidase enzyme was immobilized on a Nafion polymer film with graphene nanoplatelets [33]. It was demonstrated that such simple non-covalent bonding enhances the redox current of a ferrocyanide solution and leads to a lowering of the over potential of hydrogen peroxide[33]. In another example, direct electron transfer was observed in graphene/ionic liquid/glucose oxidase systems [34]. Other schemes for enzymatic detection of glucose have been reported using Au NPs/graphene/chitosan composites[35]. Another biosensor was developed for the detection of pesticides [36] and hydrogen peroxide (using horseradish peroxidase[37] or hemoglobin[38]).

4. Graphene Chemical Sensor

Graphene, as a new member of carbon family, has emerged as a promising candidate for sensing because of its unique electronic, excellent mechanical, chemical, and thermal properties [48-57]. Excellent sensing performance of graphene towards different kinds of gases, including NO_2, NH_3, H_2O, CO, trimethylamine, I_2, ethanol, HCN, dimethyl methylphosphonate (DMMP), and DNT, have been reported [58-64]. Generally, there are three main methods to prepare graphene materials: micromechanical exfoliation of graphite [72], chemical vapor deposition [65], and reduction of graphene oxide (GO) [66]. The resultant graphene materials can be considered as excellent candidates for gas sensing, especially for chemically reduced graphene oxide (rGO). The rGO sheets have great potential for using as chemiresistors [67-70] due to their scalable production, easy process ability in solution, large available surface area, etc. Hydrazine and ascorbic acid have been reported as excellent reducing agents for the reduction of GO, and the resultant rGO sheets show excellent responses to different vapors [59, 70]. Although many reports have been reported on the rGO sensing devices, it is still a great challenge to develop chemiresistive sensors based on rGO with miniature, low-cost, and portable characteristics.

Herein, we report a facile and controllable self-assembly technique to fabricate rGO sensors, which could be used as an excellent NH_3 gas sensing device. Negative GO sheets with large sizes (>10 µm) can be easily electrostatically attracted onto positive Au electrodes modified with cysteamine hydrochloride in aqueous solution. The assembled GO sheets on Au electrodes can be directly reduced into rGO sheets by hadrazine or pyrrole vapor and consequently provide the sensing devices based on self assembled rGO sheets. In addition, pyrrole-vapor-reduced rGO-based sensor exhibits excellent response to NH_3. We expect the easy, reproducible, green, and scalable fabrication of the sensors based on rGO reduced by pyrrole, with excellent performance, miniature, low-cost, and portable characteristics, can pave a new avenue for the application of assembled rGO devices in gas sensing field.

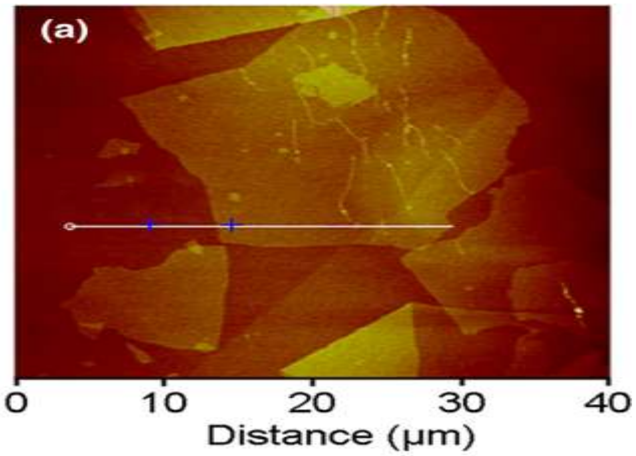

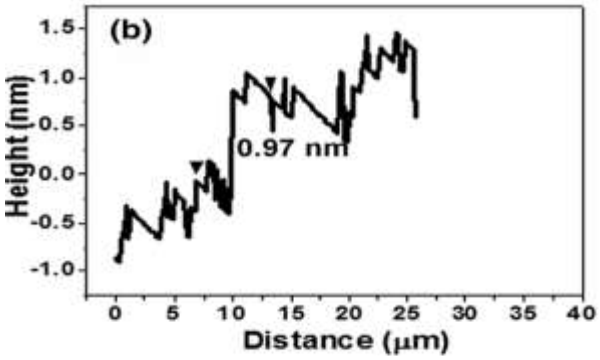

Figure 5: AFM image (a) and height profile (b) of GO sheets deposited on mica surfaces.

In order to make sure the rGO sheets bridge the gaps of the parallel Au electrodes, GO sheets with large sizes were prepared in this work. Natural graphites with large sizes (32 meshes) were used as original materials, and a modified Hummers method was exploited similar with the work reported by Zhao et al. [73]. Dialysis was carried out for the purpose of complete removal of acid in the suspension, and mild sonication was applied in order to avoid the destruction of GO sheets. As a result, single GO sheets were formed in aqueous solution and large sizes were maintained as well. The morphology of GO sheets was observed by AFM; the results were shown in Figure 6. As shown in (Figure 6a), the sizes of the majority of GO sheets were larger than 10 μm, which was in consistence with the results of SEM images of electrodes discussed later. Furthermore, the height profile of the AFM image (Figure 6b) indicated that the thickness of the obtained GO sheet was about 0.97 nm, suggesting the successful achievement of the single-layer GO sheets [75]. As we know, GO sheets contain a large number of negative functional groups (e.g., hydroxyl and carboxyl groups) [76], which can be a benefit for their electrostatic attraction with positive surfaces during the self assembly process.

Figure 6: (a) Pre-patterned electrode

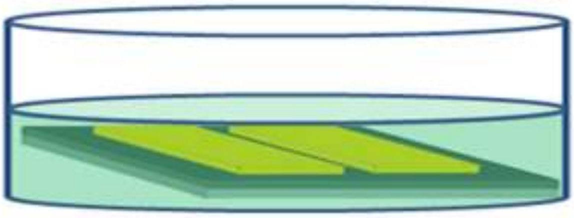

Figure 6: (b) Immersion into cysteamine hydrochloride aqueous solution

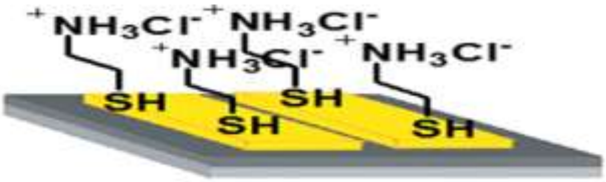

Figure 6: (c) Positive charged Au electrodes

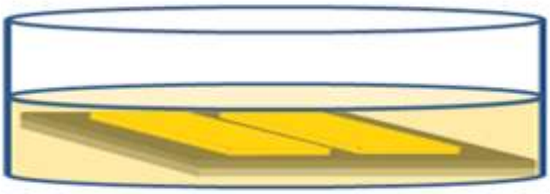

Figure 6: (d) Immersion in to negatively charged GO aqueous solution

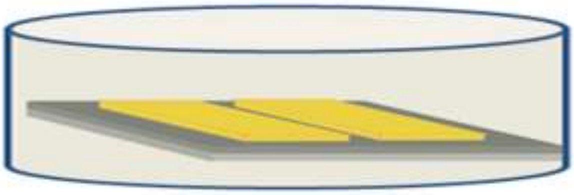

Figure 6: (e) Treated by hydrazine or pyrrole vapor

Figure 6: (f) Assembled rGO sheets based sensing device

Figure 6: Schematic illustration of the fabrication of sensing devices based on self-assembled rGO sheets.

The sensing devices were fabricated by self-assembly of the obtained GO sheets on Au electrodes, followed by in situ reduction by hydrazine or pyrrole vapor. The process was schematically illustrated in Figure 6.

The parallel Au electrodes on SiO_2 (300 nm)/Si wafers were easily patterned by a standard micro fabrication process, and the distance of the gap was fixed at about 1 μm in order to make sure GO sheets be easily bridged on between paralleled Au electrodes. Since electrostatic attraction was applied as driving forces for self-assembly of negative GO sheets on Au electrodes, Au electrodes were treated by cysteamine hydrochloride aqueous solution in advance to attach positively charged amine groups. As we know, organic molecules with thiol groups can be assembled on the surface of Au through forming self-assembled mono layers (SAMs) due to the strong affinity between sulfur and Au [77,78]. Hence, SAMs with positively charged amine groups on the surface of Au electrodes were formed during this assembly process. The resultant Au electrodes assembled with GO sheets were further put in sealed vessels and reduced by hydrazine or pyrrole vapor at 90°C the GO sheets on Au electrodes were in situ reduced into rGO and consequently formed the sensing devices based on assembled rGO sheets.

5. Graphene ph sensor

Figure 7 sketches the entire mask-free fabrication process of our graphene sensor. Graphene sheets were first made by mechanical exfoliation of bulk graphite (Kish Graphite, purchased from Graphene Supermarket) with scotch tape

Licensed Under Creative Commons Attribution CC BY

and randomly deposited onto a 285 nm SiO_2 layer on a silicon wafer (P/B(100), 1-10ohm-cmpurchased fromuniversitywafer.com). This specific SiO_2 thickness is chosen because it can provide the best visibility of graphene sheets, which can be explained by Fresnel-law-based models as developed in [79, 80]. An optical microscope and a camera (Nikon MM-40 and DXM 1200) were then used to identify and locate individual graphene sheets (as sketched in Figure 1a). This is currently the easiest and most popular way to spot graphene crystallites among copious thicker flakes. Usually,

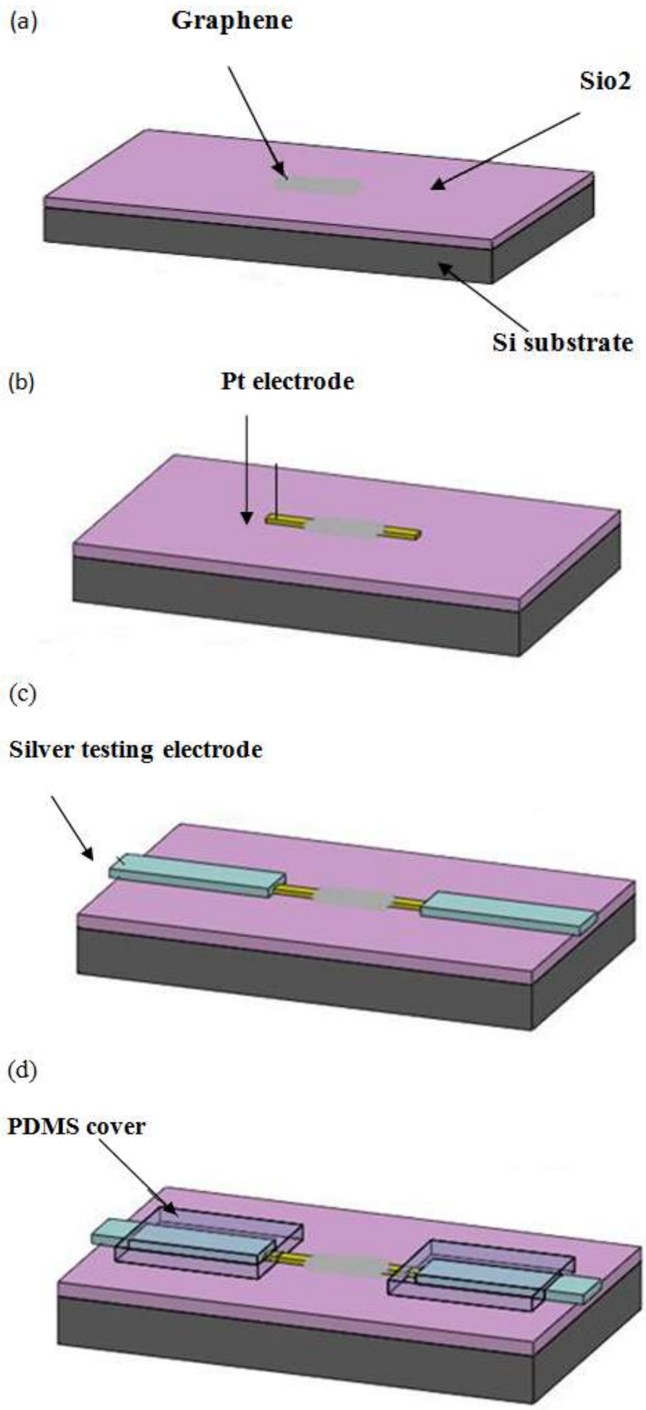

Figure 7: The mask-free fabrication process of a graphene sensor.

Figure 7a few micron-sized graphene can be found over a 4 millimeter-sized area, which is already sufficient for our purpose, because only one graphene sheet is needed on each wafer piece for device fabrication. A dual beam system (FEI Quanta 3D 200i) was used for the fabrication of electrodes and observation of the sample: an ion beam for electrode deposition and an electron beam for imaging. The area of interest on the sample was positioned at the eucentric point where the two beams cross, as shown in Figure 7a. At this location, the electron beam could provide in situ imaging of the graphene. The sample was tilted at 52° for optimized ion incident angle. The FIB employs highly-focused Pt+ ion beam scanned over the desired areas of the sample surface. The Pt metal organic precursor (methylcyclopentadienyl trimethyl platinum) is introduced by a gas-injection system during the ion beam scanning, providing the well-controlled ion-assisted deposition of the metal. Therefore, the Pt lines can be fabricated directly over the desired area of a graphene with approximately 20 nm precision. In this study, to prevent the graphene from being damaged by the Pt^+ ions, two contact electrodes (10 μm×100 nm × 100 nm) were first deposited on two sizes of graphene under 16.0 kV acceleration voltage and 4.0 pA ion current. Then, another two rectangular electrodes (200μm× 10μm × 100 nm) were deposited to expand the contact electrodes under 30.0 kV acceleration voltage and 0.5 nA ion current.

Figure 7b shows a microscopic image of the fabricated electrodes on both sides of a graphene sheet. To expand the contact platinum electrodes, two millimeter sized testing pads, as sketched in Figure 7c, were conveniently made by carefully painting a layer of silver on the wafer using high-purity conductive silver paint (SPI 05001-AB), operated under a stereo microscope (Nikon S2800). To eliminate the 5 potential contamination of silver particles from dissipating into the testing samples, a layer of polydimethylsiloxane (PDMS) (Dow Corning Sylgard 184) was carefully cured on top of the silver electrodes and leaves a 200-300μm gap large enough for future experiments on the graphene sheet. The configuration of a fabricated graphene device is sketched in Figure7d.

To perform pH sensing experiments, a wetting and drying process was used. After the resistance of the device in the air was stabilized, the first pH buffer drop was carefully placed on top of the graphene sheet as shown in Figure 8. After approximately 1~2 minutes when the resistance became stable, this pH buffer drop was carefully sucked up by vacuum, and then more buffer drops with different pH values were applied and removed repeatedly in the same way. In our experiments, buffers with pH values from 4 to 10 (standard buffer solutions from Fisher Scientific) were tested. During the experiment, the resistance of the device under 7a constant current were monitored and recorded in real time by a semiconductor analyzer.

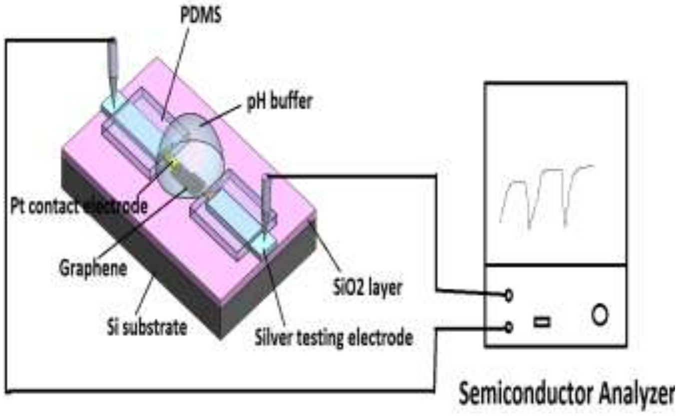

Figure 8: Configuration of the experimental system.

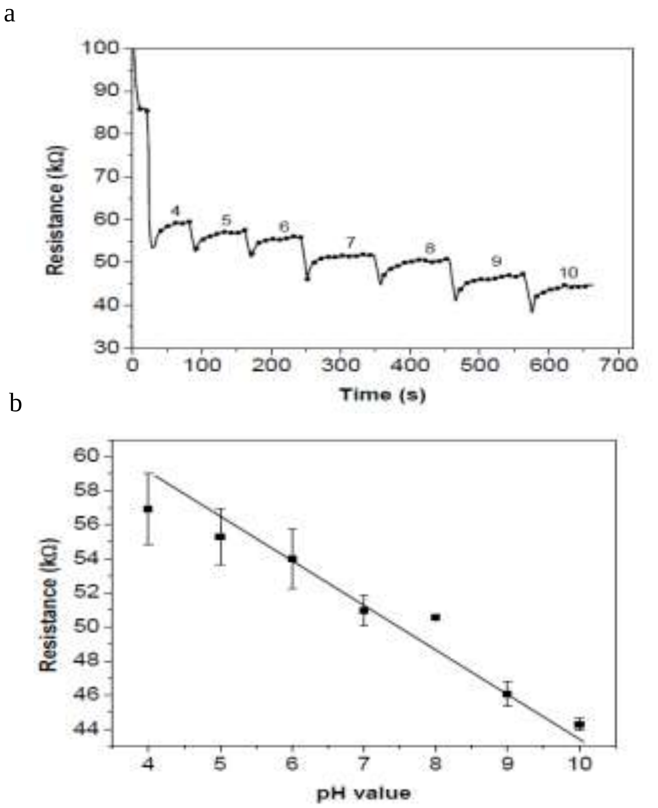

Figure 9: (a) Real-time resistance measurements of the graphene sensor when exposed to pH buffers from pH-4 to pH-10; (b) complied resistance data from multiple measurements plotted as a function of pH values.

Figure 9a reports a real time measurement of the resistance of our graphene device under a constant current at 10 μA. The resistance of the device in the air is approximately 86 kΩ When a drop of pH-4 buffer was placed on the graphene, the resistance rapidly decreased to 59.2 kΩ. The resistance is then decreased by 2.2 kΩ when pH-5 buffer was placed on the graphene. Similar amount of decrement is observed when the pH buffer was changed to pH-6, pH-7, pH-8, pH-9 and pH-10. Figure 9b shows the average values (dots) and standard deviations (error bars) of the resistance from multiple measurements on this specific device. A linear correlation can be used to describe the curve in Figure 5b: $R = (-2.13 \times \mathrm{pH} + 66.11)$ kΩ This equation indicates that the sensitivity of the particular device is 2.13 kΩ/pH [111].

6. Graphene Image Sensor

Graphene is a material composed of pure carbon with atoms arranged in a regular hexagonal pattern. It is a one-atom thick layer of the mineral graphite, a million times smaller than the thickest human hair and is known to have a high electrical conductivity and is very light, with a 1-square-meter sheet weighing only 0.77 milligrams.

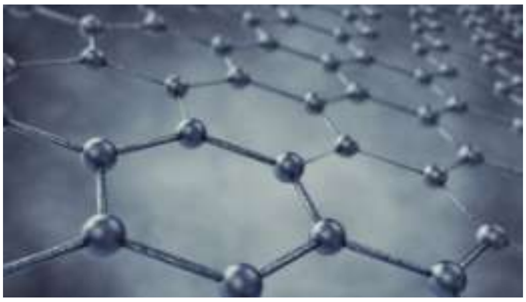

Figure 10: Graphene is the basis of the new image sensor.

Asst. Prof Wang has devised a novel way to create nanostructures on graphene which "trap" light-generated electron particles for a longer period of time, translating into a stronger electrical signal. These electrical signals are then processed into an image, such as a photograph captured by a digital camera. The "trapped electrons" are the key to achieving high photo response in graphene, which makes it far more effective than the normal CMOS or CCD image sensors, said Asst Prof Wang. Essentially, the stronger the electric signals generated, the clearer and sharper the photos. "The performance of our graphene sensor can be further improved, such as the response speed, through nanostructure engineering of graphene, and preliminary results already verified the feasibility of our concept," Asst. Prof Wang says.

A team of scientists at Nanyang Technological University (NTU) in Singapore has developed a new image sensor from graphene that promises to improve the quality of images captured in low light conditions. In tests, it has proved to be 1,000 times more sensitive to light than existing complementary metal-oxide-semiconductor (CMOS) or charge-coupled device (CCD) camera sensors in addition to operating at much lower voltages, consequently using 10 times less energy.

Camera ISO is one of the three pillars of photography (the other two being aperture and shutter speed). In simple terms, ISO is the level of sensitivity of your camera’s image sensor to available light. The majority of people taking pictures have probably never adjusted the ISO setting on their cameras so here is an explanation. Essentially, a lower ISO setting reduces your cameras sensitivity to light creating higher quality images, while a higher ISO number increases sensitivity and your camera sensor can capture images in low-light environments without having to use a flash. But higher sensitivity comes at a cost it adds grain or “noise” to the pictures. of course, not all grain is bad and we often see creative uses of it in black and white photography. But if you are a sports photographer shooting in a poorly lit indoor stadium, in order to freeze action, you have to shoot with a wide aperture (f 2.8 or lower) and try to keep your shutter

Licensed Under Creative Commons Attribution CC BY

speed above 500. The only way to do this is to increase ISO and live with the resulting grainy pictures. Asst. Professor Wang's graphene sensor, being more sensitive, will negate the need to increase ISO in low light settings [81].

7. Graphene Magnetic Field Sensor

The spatially localized detection of magnetic fields at nano scale resolution is a considerable technological challenge, with potential applications ranging from sensors for magnetic storage to bio sensing and scanning probe microscopy. The most common approaches employ magneto resistive devices fabricated from ferromagnetic materials such as GMR and TMR spin valves and Hall devices. However, as the size of the magnetic domain to be detected decreases, the magnetic spacing and the size of the sensor need to be reduced accordingly in order to maintain high spatial resolution and signal-to-noise ratio (SNR).

Graphene, a two-dimensional honeycomb lattice of carbon atoms, is a material that provides a conductive layer only one atom thick that can be located at or near a sensor surface, and has high mobility and high current carrying capabilities [82]. These characteristics uniquely position graphene as a candidate material for high spatial resolution magnetic field sensors based on the Lorentz force. devices consisting of hybrid graphene-metal structures in which the redistribution of current flowing through a metal shunt and graphene channel in a magnetic field modulates the resistance of the device[83].

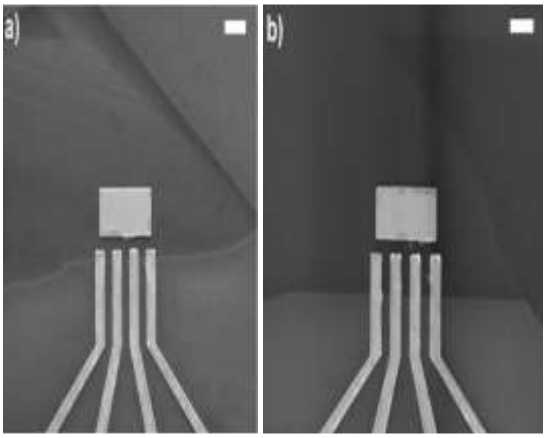

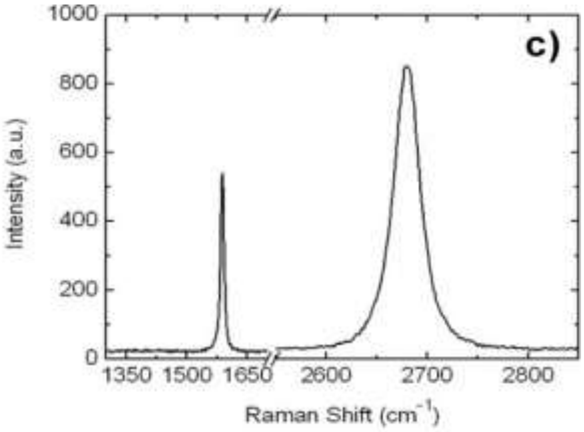

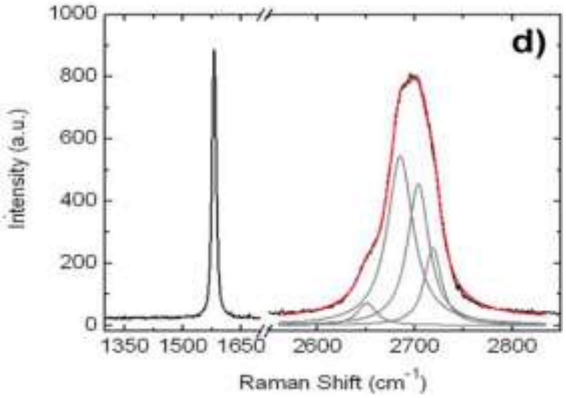

Figure 11: Single layer (a) and bilayer (b) graphene EMR devices, scale bar 500 nm. The Raman spectra at 514 nm excitation associated with devices in (a) and (b) are shown in (c) and (d) respectively. The 2-D band in the bilayer device in (d) is composed of four lorentzian components, as shown.

The graphene EMR devices were fabricated by exfoliating HOPG graphite on 1 cm n-doped crystalline Si substrates covered by 300 nm thermally grown. The low resistivity Si serves as a back gate electrode. Single layer and bilayer graphene flakes were first selected by optical microscopy and the number of layers confirmed by Raman spectroscopy [84]. The device fabrication was completed by defining electrodes and shunt by e-beam lithography through a PMMA mask, depositing Ta/Au (2.5/20 nm) and lifting-off.

Figure 11 show typical single layer and bilayer EMR devices and the associated Raman spectra. The Raman spectrum contains the G peak near 1580 cm^{-1}, associated with the zone center E_2 mode, and the 2-D peak near 2700 cm^{-1} , associated with the second order breathing mode of the bonded carbon atoms in the honeycomb lattice. The first order breathing mode, referred to as the D peak, near 1350 cm^{-1} requires a defect for its activation, and can be seen when probing the graphene flake edges or when structural defects are present. The lack of the D peak in our samples is an indication of good crystalline structure. The 2-D peak does not require defects to be Raman active and can be used to count the number of graphene layers in a flake. The presence of a single lorentzian peak (Figure 11(c)) in the 2-D band indicates single layer graphene. On the other hand, the four lorentzian components in the 2-D band in Figure 11(d) are indicative of bilayer graphene, as determined by their relative position and intensities [85].

8. Graphene Strain Sensor

Piezoresistive effect has been widely used for sensor devices employing various metals and semiconductors.[86–88] Along with the relentless pursuit of low-cost and miniaturized devices, different candidate materials have been developed including low-dimensional carbons.[89–93] Carbon nanotubes (CNTs) and graphene are two examples applicable for piezoresistive strain sensors and have attracted enormous attention in recent years. A piezoresistive sensitivity gauge factor (GF) up to 2900 has been achieved for CNTs-based strain sensors[94,95] in comparison, graphene-based strain sensors have lower sensitivity.[96–98] Compared with the quasione- dimensional structure of

CNTs, graphene is an ideal two-dimensional structure thus has advantages in scalable devices fabrication via top-down approaches, which is compatible with existing fabrication technology. Graphene, a one-atom-thick carbon honey-comb network, is one of the most stable structures and has novel electrical and mechanical properties[97–105]. For perfect graphene, its electrical conductivity could change under strain induced structural deformation thus this piezoresistive effect can be used for diverse strain sensing applications. Various graphene strain sensors have been developed so far, and the piezoresistive sensitivity, represented by the GF, of grapheme is low due to its semi-metal nature. For example, suspended graphene shows a GF 1.9 with the applied strain <3% [106] chemical vapor deposition (CVD) graphene on polydimethylsiloxane (PDMS) shows a GF of 6.1[107] and graphene ripples on PDMS shows a GF~2 with the applied strain up to 30%.[108] Semiconducting graphene may have large piezoresistive sensitivity,[88] however, the metal-to-semiconductor phase change under strain is not observed yet experimentally. Alternatively, graphene/epoxy composite has been developed with a GF~11.4 in order to increase the sensitivity of graphene-based strain sensors [109].

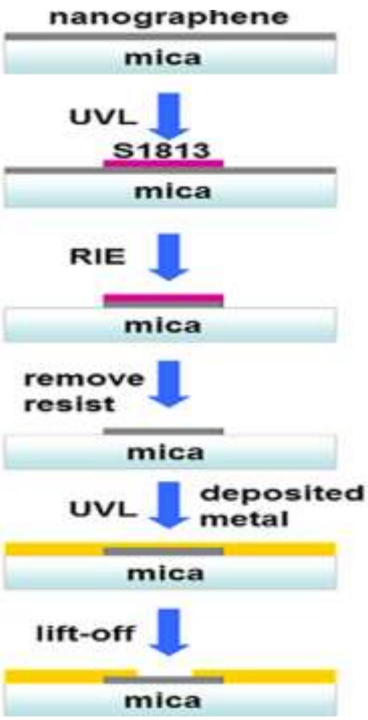

Figure 12: (a) The fabrication process of NG-based strain sensor devices.

The fabrication progress for NG strain sensors is shown in Figure 12(a). NG film on mica was used as the starting material. S1813 resist was spin-coated at 4500 rpm on the as prepared samples, and then was patterned into strips by ultraviolet (UV) lithography (MA6, Karl Suss). NG patterns were then formed by O_2-plasma etching, which was carried out in a reactive ion etching system (Plasma Lab 80 Plus, Oxford Instruments Company) using plasma power of 100 W, O_2 pressure of 0.1Torr, and etching time of 11 s, respectively. In the following step, contact electrodes were made for the patterned NG film by a second UV lithography, Ti/Au (2 nm/ 30 nm) metal deposition via e-beam evaporation, and standard lifting-off techniques. As-fabricated devices were annealed in hydrogen atmosphere at 380 ^{0} C for 1 h to improve contacts before any electrical measurements.

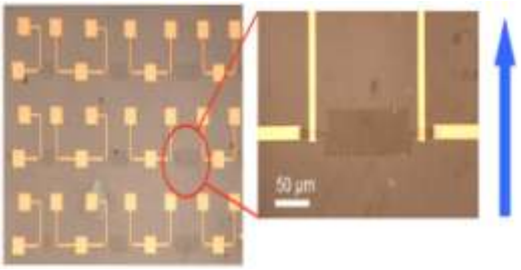

Figure 12: (b) Optical images of the as-patterned

Devices with the zoom-in image of an individual device shown on the right. The arrow marks the bending direction. The optical image of a device array was shown in Figure 12 (b) in which the zigzag-shape NG strips are 2 lm-wide and 1.4mm-long with a sheet resistance of about 5.5 MX/w. The as-made strain sensor devices were bonded by silver conducting epoxy and wired out for electrical measurements, and the applied strain was along arrow's direction (marked in Figure 12(b)) during measurements.

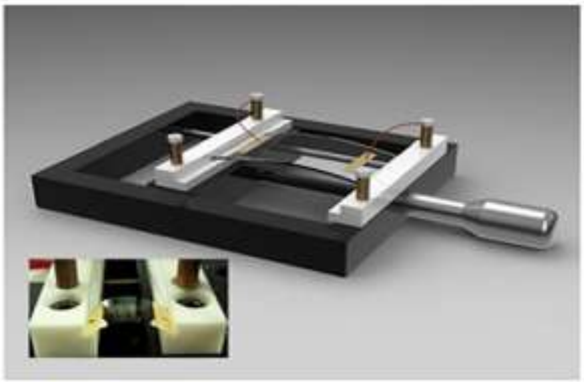

Figure 12: (c) Sketch map of the experimental setup for applying strain to devices; the inset shows an optical image of a real sample.

The experimental setup for measurements is shown in Figure 12 (c). Mica substrate with devices was mounted on a micrometer caliper, which can push the mica substrate to cause bending, and in this way the strain was applied. Note that the NG films adhere to mica firmly due to strong vander Waals force and no fracture failure was observed in all measurements below a compressing or tensile strain less than 0.5%. The bending direction is always along the vertical direction marked in Figure 12 (b).

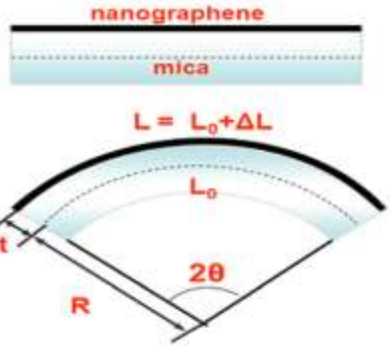

Figure 12: (d) Illustration of a mica substrate.

Licensed Under Creative Commons Attribution CC BY

under bending Figure 12 (d) illustrates the bending of the mica substrate. As 2Rh $^{\theta}$ L0 and 2Rsinh $^{\theta}$L .where L0 and L represent the length before and after deformation, respectively; and DL$^{\theta}$L0-L. R is radius of curvature and Dt is half of the thickness of the mica substrate. The corresponding electrical properties were measured at ambient conditions by semiconductor parameter analyzer (Agilent 4156C) [110].

9. Conclusion

Graphene is very high electric conductivity, carrier mobility, thermal conductivity, Mechanical properties, flexibility, and chemical properties transparent cheekily and all other factor of the graphene is excellent then other material and this graphene properties and factors very match to development high efficiency, flexible, low cost and sensitive sensor technology.

References

[1] Georgakilas V, Otyepka M, Bourlinos AB, Chandra V, Kim N, et al. (2012) Functionalization of Graphene: Covalent and non-covalent approaches, derivatives and applications. Chem Rev 112: 6156-6214

[2] Lee C, Wei X, Kysar JW, Hone J. Measurement of the elastic properties and intrinsic strength of monolayer graphene. Science 2008;321(5887):385–8.

[3] Kim BJ, Jang H, Lee S-K, Hong BH, Ahn J-H, Cho JH.High-performance flexible graphene field effect transistors with ion gel gate dielectrics. Nano Lett 2010;10(9):3464–6.

[4] Liu Z, Liu Q, Huang Y, Ma Y, Yin S, Zhang X, et al. Organic photovoltaic devices based on a novel acceptor material: graphene. Adv Mater 2008;20(20):3924–30.

[5] Han T-H, Lee Y, Choi M-R, Woo S-H, Bae S-H, Hong BH, et al. Extremely efficient flexible organic light-emitting diodes with modified graphene anode. Nat Photon 2012;6(2): 105–10.

[6] Wang Y, Tong SW, Xu XF, O¨ zyilmaz B, Loh KP. Interface engineering of layer-by-layer stacked graphene anodes for high-performance organic solar cells. Adv Mater 2011;23(13):1514–8.

[7] Kim R-H, Bae M-H, Kim DG, Cheng H, Kim BH, Kim D-H, et al. Transparent graphene interconnects for arrays of microscale inorganic light emitting diodes on rubber substrates. Nano Lett 2011;11(9):3881–6.

[8] K. V. Emtsev, A. Bostwick, K. Horn, J. Jobst, G. L. Kellogg, L. Ley, J. L. McChesney, T. Ohta, S. A. Reshanov, J. Rohrl, E. Rotenberg, A. K. Schmid, D. Waldmann, H. B. Weber, and

[9] T. Seyller. Towards wafer-size graphene layers by atmospheric pressure graphitization of silicon carbide. Nat. Mater., 8(3):203–207, 2009. doi: 10.1038/NMAT2382.

[10] K. S. Kim, Y. Zhao, H. Jang, S. Y. Lee, J. M. Kim, K. S. Kim, J.-H. Ahn, P. Kim, J.-Y. Choi, and B. H. Hong. Large-scale pattern growth of graphene films for stretchable transparent electrodes. Nature, 457(7230):706–710, February 2009. doi: 10.1038/nature07719.

[11] S. Park and R. S. Ruoff. Chemical methods for the production of graphenes. Nat. Nano., 4(4): 217–224, April 2009. doi: 10.1038/nnano.2009.58.

[12] L. Chen, Y. Hernandez, X. Feng, and K. M¨ullen. From Nanographene and Graphene Nanoribbonsto Graphene Sheets: Chemical Synthesis. Angew. Chem. Int. Ed., 51(31):7640–7654, 2012. doi: 10.1002/anie.201201084.

[13] M. Hilder, B. Winther-Jensen, D. Li, M. Forsyth, and D. R. MacFarlane. Direct electrodeposition of graphene from aqueous suspensions. Phys. Chem. Chem. Phys., 13(20):9187–9193, 2011. doi: 10.1039/C1CP20173E.

[14] C. D. Simpson, J. D. Brand, A. J. Berresheim, L. Przybilla, H. J. R¨ader, and K. M¨ullen. Synthesis of a Giant 222 Carbon Graphite Sheet. Chem.–Eur. J., 8(6):1424–1429, 2002. doi: 10.1002/1521-3765(20020315)8:6¡1424::AID-CHEM1424¿3.0.CO;2-Z.

[15] M. J. McAllister, J.-L. Li, D. H. Adamson, H. C. Schniepp, A. A. Abdala, J. Liu, M. Herrera- Alonso, D. L. Milius, R. Car, R. K. Prud'homme, and I. A. Aksay. Single Sheet Functionalized Graphene by Oxidation and Thermal Expansion of Graphite. Chem. Mater., 19(18):4396–4404, May 2007. doi: 10.1021/cm0630800.

[16] L. J. Cote, R. Cruz-Silva, and J. Huang. Flash Reduction and Patterning of Graphite Oxide and Its Polymer Composite. J. Am. Chem. Soc., 131(31):11027–11032, July 2009. doi: 10.1021/ja902348k.

[17] E. C. Salas, Z. Sun, A. Luettge, and J. M. Tour. Reduction of Graphene Oxide via Bacterial Respiration. ACS Nano, 4(8):4852–4856, July 2010. doi: 10.1021/nn101081t.

[18] A. Turchanin, A. Beyer, C. T. Nottbohm, X. H. Zhang, R. Stosch, A. Sologubenko, J. Mayer, P. Hinze, T. Weimann, and A. Golzhauser. One Nanometer Thin Carbon Nanosheets with Tunable Conductivity and Stiffness. Adv. Mater.,21(12):1233–+,2009.doi: 10.1002/adma.200803078.

[19] A. Turchanin, D. Weber, M. B¨uenfeld, C. Kisielowski, M. V. Fistul, K. B. Efetov, T. Weimann, R. Stosch, J. Mayer, and A. G¨olzh¨auser. Conversion of Self-Assembled Monolayers into Nanocrystalline Graphene: Structure and Electric Transport. ACS Nano, 5(5):3896–3904, 2011. doi:10.1021/nn200297n.

[20] A. K. Geim. Nobel Lecture: Random walk to graphene. Rev. Mod. Phys., 83(3):851–862, August 2011. doi:10.1103/RevModPhys.83.851.

[21] Hulanicki, A., et al. Pure Appl Chem (1991) 63, 1247.

[22] Szabo, T., et al., Chem Mater (2006) 18, 2740.

[23] Dreyer, D. R., et al., Chem Soc Rev (2010) 39, 228.

[24] Gomez-Navarro, C., et al., Nano Lett (2010) 10, 1144.

[25] Davis, T. J., et al. Angew Chem Int Ed (2005) 44, 5251.

[26] Gao, W., et al. Nat Chem (2009) 1, 403

[27] Bonanni, A., and Pumera M., ACS Nano (2011) 5, 2356.

[28] Pumera, M., Chem Soc Rev (2010) 39, 4146.

[29] Pumera, M., et al. Trends Anal Chem (2010) 29, 954.

[30] Wilson, G. S., and Hu, Y., Chem Rev (2000) 100, 2693.

Licensed Under Creative Commons Attribution CC BY

[31] Lu, J., et al., Chem Mater (2007) 19, 6240.
[32] Wang, Y., et al., ACS Nano (2010) 4, 1790.
[33] Fu, C., et al., Electrochem Commun (2009) 11, 997.
[34] Shan, C., et al., Anal Chem (2009) 81, 2378.
[35] Shan, C., et al, Biosens Bioelectronics (2010) 25, 1070.
[36] Choi, B. G., et al. ACS Nano (2010) 4, 2910.
[37] Lu, Q., et al, Talanta (2010) 82, 1344.
[38] Xu, H., et al., Talanta (2010) 81, 334.
[39] D.R. Theavenot, K. Toth, R.A. Durst, G.S. Wilson, Pure Appl. Chem. 71 (1999) 2333.
[40] Y. Wang, Y. Li, L. Tang, J. Lu, J. Li, Electrochem. Commun. 11 (2009) 889.
[41] Y.-R. Kim, S. Bong, Y.-J. Kang, Y. Yang, R.K. Mahajan, J.S. Kim, H. Kim, Biosens. Bioelectron. 25 (2010) 2366.
[42] J. Li, S. Guo, Y. Zhai, E. Wang, Electrochem. Commun. 11 (2009) 1085.
[43] J. Li, S. Guo, Y. Zhai, E. Wang, Anal. Chim. Acta 649 (2009) 196.
[44] M. Pumera, R. Scipioni, H. Iwai, T. Ohno, Y. Miyahara, M. Boero, Chem. Eur. J. 15 (2009) 10851.
[45] C. Shan, H. Yang, J. Song, D. Han, A. Ivaska, L. Niu, Anal. Chem. 81 (2009) 2378.
[46] Y. Wang, Y. Shao, D.W. Matson, J. Li, Y. Lin, ACS Nano 4 (2010) 1790.
[47] S. Bong, Y.-R. Kim, I. Kim, S. Woo, S. Uhm, J. Lee, H. Kim, Electrochem. Commun. 12 (2010) 129.
[48] T.T. Baby, S.S.J. Aravind, T. Arockiadoss, R.B. Rakhi, S. Ramaprabhu, Sens. Actuators, B 145 (2010) 71.
[49] Wu W, Liu Z, Jauregui LA, Yu Q, Pillai R, Cao H, Bao J, Chen YP, Pei SS: Wafer-scale synthesis of graphene by chemical vapor deposition and its application in hydrogen sensing. Sens Actuators B 2010, 150:296–300.
[50] Pearce R, Iakimov T, Andersson M, Hultman L, Lloyd Spetz A, Yakimova R: Epitaxially grown graphene based gas sensors for ultrasensitive NO2 detection. Sens Actuators B 2011, 155:451–455.
[51] Joshi RK, Gomez H, Alvi F, Kumar A: Graphene films and ribbons for sensing of O2, and 100 ppm of CO and NO2 in practical conditions. J Phys Chem C 2010, 114:6610–6613.
[52] Song H, Zhang L, He C, Qu Y, Tian Y, Lv Y: Graphene sheets decorated with SnO2 nanoparticles: in situ synthesis and highly efficient materials for cataluminescence gas sensors. J Mater Chem 2011, 21:5972–5977.
[53] Du D, Liu J, Zhang X, Cui X, Lin Y: One-step electrochemical deposition of a graphene-ZrO2 nanocomposite: preparation, characterization and application for detection of organophosphorus agents. J Mater Chem 2011, 21:8032–8037.
[54] Ratinac KR, Yang W, Ringer SP, Breat F: Toward ubiquitous environmental gas sensors-capitalizing on the promise of graphene. Environ Sci Technol 2010, 44:1167–1176.
[55] Jeong HY, Lee DS, Choi HK, Lee DH, Kim JE, Lee JY, Lee WJ, Kim SO, Choi SY: Flexible room-temperature NO2 gas sensors based on carbon nanotubes/reduced graphene hybrid films. Appl Phys Lett 2010, 96:213105. 1–3.
[56] Novoselov KS, Geim AK, Morozov SV, Jiang D, Zhang Y, Dubonos SV, Grigorieva IV, Firsov AA: Electric field effect in atomically thin carbonfilms. Science 2004, 306:666–669.
[57] Yang Z, Gao R, Hu N, Chai J, Cheng Y, Zhang L, Wei H, Kong ESW, Zhang Y: The prospective 2D graphene nanosheets: preparation, functionalization and applications. Nano-Micro Letters 2012, 4:1–9.
[58] Sun X, Gong Z, Cao Y, Wang X: Acetylcholiesterase biosensor based on poly(diallyldimethylammonium chloride)-multi-walled carbon nanotubes-graphene hybrid film. Nano-Micro Letters 2013, 5:47–56.
[59] Schedin F, Geim AK, Morozov SV, Hill EW, Blake P, Katsnelson MI, Novoselov KS: Detection of individual gas molecules adsorbed on graphene. Nat Mater 2007, 6:652–655.
[60] Robinson JT, Perkins FK, Snow ES, Wei ZQ, Sheehan PE: Reduced graphene oxide molecular sensors. Nano Lett 2008, 8:3137–3140.
[61] Arsat R, Breedon M, Shafiei M, Spizziri PG, Gilje S, Kaner RB, Kalantar-zadeh K, Wlodarski W: Graphene-like nano-sheets for surface acoustic wave gas sensor applications. Chem Phys Lett 2009, 467:344–347.
[62] Jung I, Dikin D, Park S, Cai W, Mielke SL, Ruoff RS: Effect of water vapor on electrical properties of individual reduced graphene oxide sheets. J Phys Chem C 2008, 112:20264–20268.
[63] Qazi M, Koley G: NO2 detection using microcantilever based potentiometry. Sensors 2008, 8:7144–7156.
[64] Hwang EH, Adam S, Das Sarma S: Transport in chemically doped graphene in the presence of adsorbed molecules. Phys Rev B 2007, 76:195421. 1–6.
[65] Yuan W, Shi G: Graphene-based gas sensors. J Mater Chem A 2013, 1:10078–10091.
[66] Yuan W, Liu A, Huang L, Li C, Shi G: High-performance NO2 sensors based on chemically modified graphene. Adv Mater 2013, 25:766–771.
[67] Zhang Y, Zhang L, Zhou C: Review of chemical vapor deposition of graphene and related applications. Acc Chem Res 2013, 46:2329–2339.
[68] Park S, Ruoff RS: Chemical methods for the production of graphenes. Nat Nanotechnol 2009, 4:217–224.
[69] Hu N, Wang Y, Chai J, Gao R, Yang Z, Kong ESW, Zhang Y: Gas sensor based on p-phenylenediamine reduced graphene oxide. Sens Actuators B 2012, 163:107–114.
[70] Vedala H, Sorescu DC, Kotchey GP, Star A: Chemical sensitivity of graphene edges decorated with metal nanoparticles. Nano Lett 2011, 11:2342–2347.
[71] Myers M, Cooper J, Pejcic B, Baker M, Raguse B, Wieczorek L: Functionalized graphene as an aqueous phase chemiresistor sensing material. Sens Actuators B 2011, 155:154–158.
[72] Lu GH, Park S, Yu KH, Ruoff RS, Ocola LE, Rosenmann D, Chen JH: Toward practical gas sensing using highly reduced graphene oxide: a new signal processing method to circumvent run-to-run and device-to-device variations. ACS Nano 2011, 5:1154–1164.

Licensed Under Creative Commons Attribution CC BY

[73] Dua V, Surwade SP, Ammu S, Agnihotra SR, Jain S, Roberts KE, Park S, Ruoff RS, Manohar SK: All-organic vapor sensor using inkjet-printed reduced graphene oxide. Angew Chem Int Ed 2010, 49:2154–2157.

[74] Novoselov KS, Geim AK, Morozov SV, Jiang D, Zhang Y, Dubonos SV, Grigorieva IV, Firsov AA: Electric field effect in atomically thin carbon films. Science 2004, 306:666–669.

[75] Zhao J, Pei S, Ren W, Gao L, Cheng HM: Efficient preparation of large-area graphene oxide sheets for transparent conductive films. ACS Nano 2010, 4:5245–5252.

[76] Wang Y, Hu N, Zhou Z, Xu D, Wang Z, Yang Z, Wei H, Kong ESW, Zhang Y: Single-walled carbon nanotube/cobalt phthalocyanine derivative hybrid material: preparation, characterization and its gas sensing properties. J Mater Chem 2011, 21:3779–3787.

[77] Stankovich S, Dikin DA, Dommett GHB, Kohlhaas KM, Zimney EJ, Stach EA, Piner RD, Nguyen ST, Ruoff RS: Graphene-based composite materials. Nature 2006, 442:282–286.

[78] Hu N, Wei L, Wang Y, Gao R, Chai J, Yang Z, Kong ESW, Zhang Y: Graphene oxide reinforced polyimide nanocomposites via in situ polymerization. J Nanosci Nanotechnol 2012, 12:173–178.

[79] Yang J, Kim J-W, Shin HS: Facile method for rGO field effect transistor: selective adsorption of rGO on SAM-treated gold electrode by electrostatic attraction. Adv Mater 2012, 24:2299–2303.

[80] Sahoo RR, Patnaik A: Surface confined self-assembled fullerene nanostructures: a microscopic study. Appl Surf Sci 2005, 245:26–38.

[81] Blake, P., E.W. Hill, A.H.C. Neto, K.S. Novoselov, D. Jiang, R. Yang, T.J. Booth, and A.K. Geim, Making graphene visible. Applied Physics Letters, 2007. 91(6): p. 063124-3.

[82] Roddaro, S., P. Pingue, V. Piazza, V. Pellegrini, and F. Beltram, The optical visibility of graphene: Interference colors of ultrathin graphite on sio2. Nano Letters, 2007. 7(9): p. 2707-2710.

[83] Graphene-based image sensor to enhance low-light photography By Colin Dunjohn May 30, 2013.

[84] A. K. Geim and K. S. Novoselov, “The rise of graphene,” Nat. Mater., vol. 6, pp. 183–191.

[85] T. D. Boone, N. Smith, L. Folks, J. A. Katine, E. E. Marinero, and B. A. Gurney, “Mesoscopic EMR device magnetic sensitivity in I-V-I-V configuration,” IEEE Electron Device Lett., vol. 30, pp. 117–119.

[86] A. C. Ferrari, J. C. Meyer, V. Scardaci, C. Casiraghi, M. Lazzeri, F. Mauri, S. Piscanec, D. Jiang, K. S. Novoselov, S. Roth, and A. K. Geim, “Raman spectrum of graphene and graphene layers,” Phys. Rev. Lett., vol. 97, p. 187401.

[87] J.-C. Charlier, P. C. Eklund, J. Zhu, and A. C. Ferrari, “Electron and phonon properties of graphene: Their relationship with carbon nanotubes,” in Carbon Nanotubes, A. Jorio, G. Dresselhaus, and M. S. Dresselhaus, Eds. Berlin: Springer-Verlag, vol. 111, Topics Appl. Physics, pp. 673–709.

[88] D.Bernstein, C. Godfrey, A. Klein, and W. Shimmin, Behaviour of Dense Media Under High Dynamic Pressures (Gordon and Breach, New York, 1968), Vol. 35, p. 461.

[89] J. C. F. Millett, N. K. Bourne, and Z. Rosenberg, J. Phys. D: Appl. Phys. 29, 2466 (1996).

[90] A. A. Barlian, W. T. Park, J. R. Mallon, A. J. Rastegar, and B. L. Pruitt, Proc. IEEE 97, 513 (2009).

[91] M. R. Werner and W. R. Fahrner, IEEE Trans. Ind. Electron. 48, 249 (2001).

[92] T. W. Tombler, C. W. Zhou, L. Alexseyev, J. Kong, H. J. Dai, L. Lei, C. S. Jayanthi, M. J. Tang, and S. Y. Wu, Nature 405, 769 (2000).

[93] J. Cao, Q. Wang, and H. J. Dai, Phys. Rev. Lett. 90, 157601 (2003).

[94] R. J. Grow, Q. Wang, J. Cao, D. W. Wang, and H. J. Dai, Appl. Phys. Lett. 86, 093104 (2005).

[95] P. Dharap, Z. L. Li, S. Nagarajaiah, and E. V. Barrera, Nanotechnology 15, 379 (2004).

[96] S. Iijima and T. Ichihashi, Nature 363, 603 (1993).

[97] C. Stampfer, A. Jungen, R. Linderman, D. Obergfell, S. Roth, and C. Hierold, Nano Lett. 6, 1449 (2006).

[98] T. Yu, Z. H. Ni, C. L. Du, Y. M. You, Y. Y. Wang, and Z. X. Shen, J. Phys. Chem. C 112, 12602 (2008).

[99] M. L. Teague, A. P. Lai, J. Velasco, C. R. Hughes, A. D. Beyer, M. W. Bockrath, C. N. Lau, and N. C. Yeh, Nano Lett. 9, 2542 (2009).

[100] C. C. Chen, W. Z. Bao, J. Theiss, C. Dames, C. N. Lau, and S. B. Cronin, Nano Lett. 9, 4172 (2009).

[101] A. K. Geim and K. S. Novoselov, Nature Mater. 6, 183 (2007).

[102] K. S. Novoselov, A. K. Geim, S. V. Morozov, D. Jiang, M. I. Katsnelson, I. V. Grigorieva, S. V. Dubonos, and A. A. Firsov, Nature 438, 197 (2005).

[103] A. K. Geim, Science 324, 1530 (2009).

[104] M. I. Katsnelson, Mater. Today 10, 20 (2007).

[105] K. S. Novoselov, A. K. Geim, S. V. Morozov, D. Jiang, Y. Zhang, S. V. Dubonos, I. V. Grigorieva, and A. A. Firsov, Science 306, 666 (2004).

[106] J. S. Bunch, A. M. van der Zande, S. S. Verbridge, I. W. Frank, D. M. Tanenbaum, J. M. Parpia, H. G. Craighead, and P. L. McEuen, Science 315, 490 (2007).

[107] C. Lee, X. D. Wei, J. W. Kysar, and J. Hone, Science 321, 385 (2008).

[108] M. Y. Huang, T. A. Pascal, H. Kim, W. A. Goddard, and J. R. Greer, Nano Lett. 11, 1241 (2011).

[109] Y. Lee, S. Bae, H. Jang, S. Jang, S. E. Zhu, S. H. Sim, Y. I. Song, B. H. Hong, and J. H. Ahn, Nano Lett. 10, 490 (2010).

[110] Y. Wang, R. Yang, Z. W. Shi, L. C. Zhang, D. X. Shi, E. Wang, and G. Y. Zhang, ACS Nano 5, 3645 (2011).

[111] Y. J. Kim, J. Y. Cha, H. Ham, H. Huh, D. S. So, and I. Kang, Curr. Appl. Phys. 11, S350 (2011).

[112] Jing Zhao, Congli He, Rong Yang, Zhiwen Shi, Meng Cheng Ultra-sensitive strain sensors based on piezoresistive nanographene films.101,063112(2012); doi: 10.1063/1.4742331

[113] Nan Lei, Pengfei Li, Wei Xue, Jie Xu, Simple graphene chemiresistors as pH sensors: fabrication and characterization , Mechanical Engineering, Washington State University, Vancouver, WA 98686, USA

Licensed Under Creative Commons Attribution CC BY